

Synthesis and properties of nicked dumbbell and dumbbell DNA conjugates having stilbenedicarboxamide linkers

Ligang Zhang, Hai Long, George C. Schatz and Frederick D. Lewis*

Received 6th October 2006, Accepted 21st November 2006

First published as an Advance Article on the web 13th December 2006

DOI: 10.1039/b614572h

The synthesis and properties of nicked dumbbell and dumbbell DNA conjugates having A-tract base pair domains connected by rod-like stilbenedicarboxamide linkers are reported. The nicked dumbbells have one to eight dA–dT base pairs and are missing a sugar–phosphate bond either between the linker and a thymine nucleoside residue or between two thymine residues. Chemical ligation of all of the nicked dumbbells with cyanogen bromide affords the dumbbell conjugates in good yield, providing the smallest mini-dumbbells prepared to date. The dumbbells have exceptionally high thermal stability, whereas the nicked dumbbells are only marginally more stable than the hairpin structures on either side of the nick. The structures of the nicked dumbbells and dumbbells have been investigated using a combination of circular dichroism spectroscopy and molecular modeling. The base pair domains are found to adopt normal B'-DNA geometry and thus provide a helical ruler for studies of the distance and angular dependence of electronic interactions between the chromophore linkers.

Introduction

Bis(oligonucleotide) conjugates having synthetic linkers connecting short complementary base pair domains can form stable DNA or RNA hairpin structures. The rod-like stilbenedicarboxamide linker SA (Chart 1a), initially reported by Letsinger and Wu,¹ forms stable hairpin structures (Chart 1b) possessing as few as three A–T base pairs or two G–C base pairs.¹ We subsequently observed that the addition of a second SA as a capping group results in a further increase in thermal stability for capped hairpin structures (Chart 1b), permitting the formation of compact folded structures possessing a single A–T base pair.²

We have employed capped hairpins with (A–T)_n base pair domains (A-tracts) to investigate the distance and angular dependence of exciton coupling,^{2,3} energy transfer,⁴ and electron transfer⁵ between hairpin linker and capping chromophores. Experimental results and molecular modeling are consistent with π -stacked structures with restricted conformational mobility for the capping chromophore. In order to confirm this proposal we sought to “fix” the conformation of the capping chromophore by removal of the nick between the chromophore and base pair domain. We report here the preparation and chemical ligation of nicked dumbbells (Chart 1c) as a method for the efficient synthesis of synthetic dumbbell structures possessing (A–T)_n base pair domains connected by the synthetic SA linkers. The properties of both the nicked dumbbells and dumbbells are dependent upon the number of base pairs. The melting temperatures of the nicked dumbbells are lower than those of either hairpin or capped hairpin structures having the same number of base pairs, whereas the dumbbells are highly resistant to melting. CD spectra are sensitive to the presence/absence of a nick and the number of base pairs. Comparison of the calculated nicked dumbbell and dumbbell

structures indicates that the presence of the nick has little effect upon duplex geometry.

Results

Syntheses of nicked dumbbells and dumbbells

The nicked dumbbells *nN* (*n* = 1–6, 8, Chart 1c) were prepared by means of conventional phosphoramidite chemistry.¹ They were purified by HPLC and characterized by UV and CD spectroscopy and by MALDI-TOF mass spectrometry. Chemical ligation of the nicked dumbbell with CNBr followed the procedure of Carriero and Damha (see Experimental section).⁶ The progress of the ligation reactions of *nN* (*n* = 1–5) was monitored by HPLC and the resulting dumbbells purified by HPLC. HPLC traces for **1N** after ligation with and without added starting material are shown in Fig. 1. Conversions of nicked dumbbell to dumbbell conjugates were 67–94%, as determined by analytical HPLC. Preparative HPLC yields were 60–85%. In the cases of **6N** and **8N** the nicked dumbbell and dumbbell had similar HPLC retention times, necessitating use of denaturing PAGE gels for dumbbell purification (Fig. 2).

Electronic absorption spectra and thermal dissociation profiles

The UV absorption spectra of the nicked dumbbells *nN* and dumbbells *nD* are shown in Fig. 3. The long-wavelength bands of the SA-linked conjugates are assigned to the allowed π,π^* transition of stilbene linker SA.⁷ These bands are red-shifted by ca. 10 nm in the conjugates vs. the stilbene linker. The bands for **1N** and **1D** are slightly blue-shifted compared to the conjugates with longer base pair domains, as previously observed for a capped hairpin having a single A–T base pair.² The 260 nm band is assigned to the overlapping absorption of the nucleobases and the weaker stilbene absorption. The 260/335 nm absorbance ratio increases with the ratio of the number of base pairs to stilbenes

Department of Chemistry, Northwestern University, Evanston, Illinois, 60208-3113, USA. E-mail: fdl@northwestern.edu

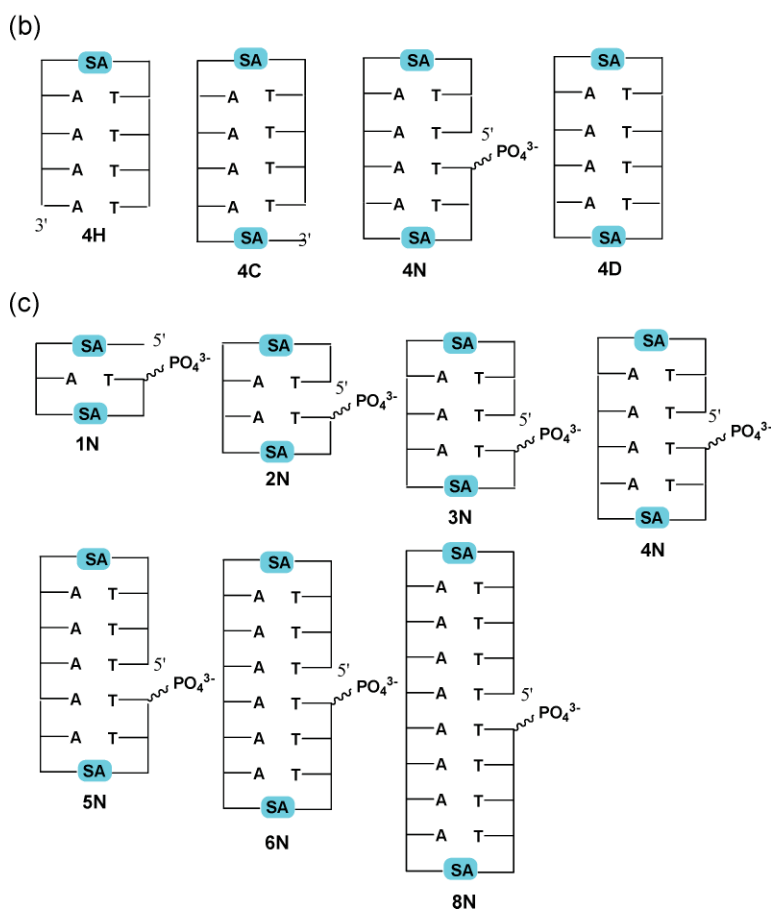
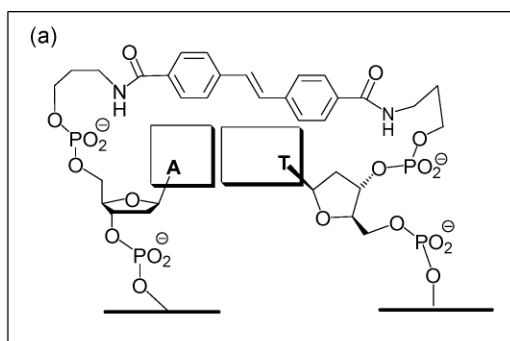


Chart 1 (a) Structure of the hairpin loop region of synthetic hairpins having a stilbenedicarboxamide (SA) linker. (b) Schematic structures of a hairpin (H), capped hairpin (C), nicked dumbbell (N), and dumbbell (D) conjugates having four dA–dT base pairs connected by a SA linker. (c) Schematic structures of nicked dumbbells having 1–6 and 8 A–T base pairs.

within the conjugate structure. The 260 nm band is also blue shifted as the number of base pairs increases from 1 to 4, as previously observed for the capped hairpins.² No shift in the absorption maxima is observed for $n > 4$ for either nicked dumbbells or dumbbells.

Thermal dissociation profiles for the nicked dumbbell and dumbbell conjugates in 10 mM phosphate buffer determined at 260 nm using a Peltier temperature controller with a heating rate of $0.5\text{ }^{\circ}\text{C min}^{-1}$ are shown in Fig. 4. Hyperchromism is observed for

the 260 nm bands of all of the SA-linked conjugates. Conjugates 1N and 2N do not have well-defined melting transitions, even with added 0.1 M NaCl. Melting temperatures determined from the derivatives of these profiles are reported in Table 1, along with values of T_m obtained for several of the nicked dumbbells with added 0.1 M NaCl. All of the SA-linked dumbbells have T_m values $> 80\text{ }^{\circ}\text{C}$ and thus the reported values are not highly accurate. Also reported in Table 1 are the values of T_m for the corresponding hairpins and capped hairpins.²

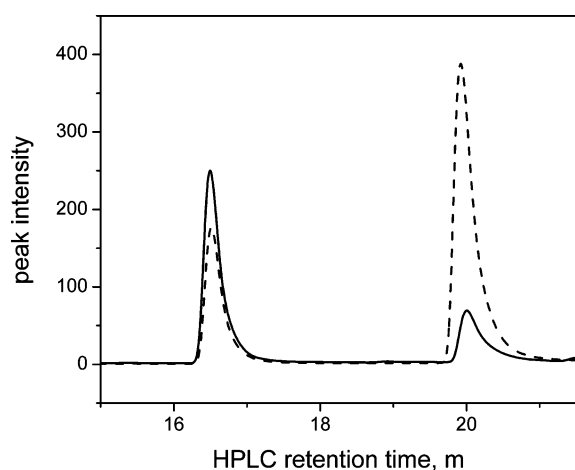


Fig. 1 HPLC trace of ligated product mixture obtained from **1N** (solid line) and product mixture after addition of unligated starting material (dashed line).

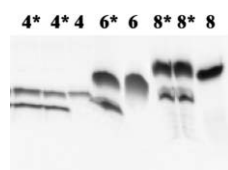


Fig. 2 Denaturing gel of nicked dumbbells **nN** ($n = 4, 6,$ and 8) and their corresponding ligation mixtures (tracks indicated by asterisk).

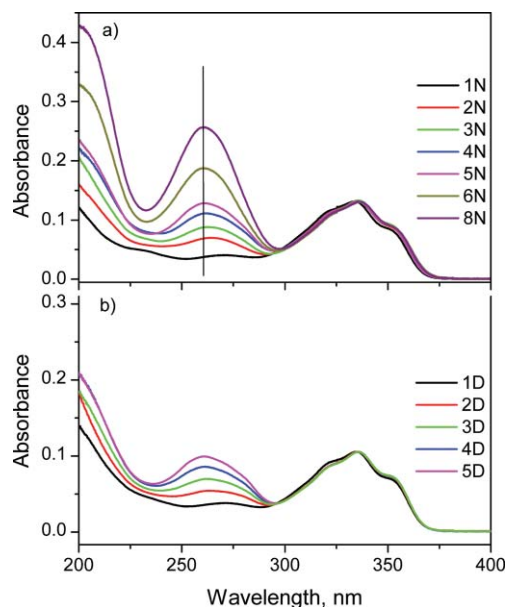


Fig. 3 UV spectra of (a) nicked dumbbells **nN** ($n = 1-6$ and 8) and dumbbells **nD** ($n = 1-5$) in aqueous solution (ca. $5 \mu\text{M}$ conjugate, 10 mM sodium phosphate buffer).

Circular dichroism spectra

The CD spectra of the nicked dumbbells **nN** and dumbbells **nD** ($n = 1-4$) are shown in Fig. 5 along with the previously published spectra for the capped hairpins **nC** (Chart 1b). The CD bands in the $290-350 \text{ nm}$ spectral region are attributed to exciton coupling

Table 1 Melting temperatures ($^{\circ}\text{C}$) for hairpins, capped hairpins, nicked dumbbells, and dumbbells^a

n	$n\text{H}^b$	$n\text{C}^c$	$n\text{N}^{d,e}$	$n\text{D}^d$
1		48.9		>80
2		62.6		91
3	42	63.8	36(42)	91
4	49	67.6	37	88
5		70.1	40	88
6	59	72.1	42(50)	84
8		72.5	45(56)	84

^a Structures shown in Chart 1b, $n =$ number of base pairs. ^b Data from ref. 1 for $1.0 A_{260} \text{ unit mL}^{-1}$ in 10 mM TrisHCl, pH 7, with 0.1 M NaCl. ^c Data from ref. 2 for capped hairpins in sodium phosphate buffer containing 0.1 M NaCl. ^d Data for $5 \mu\text{M}$ solutions (10 mM sodium phosphate buffer, pH 7.2, no added salt) obtained with a heating rate of $0.5 \text{ }^{\circ}\text{C}$. ^e Values in parentheses for solutions containing 0.1 M NaCl.

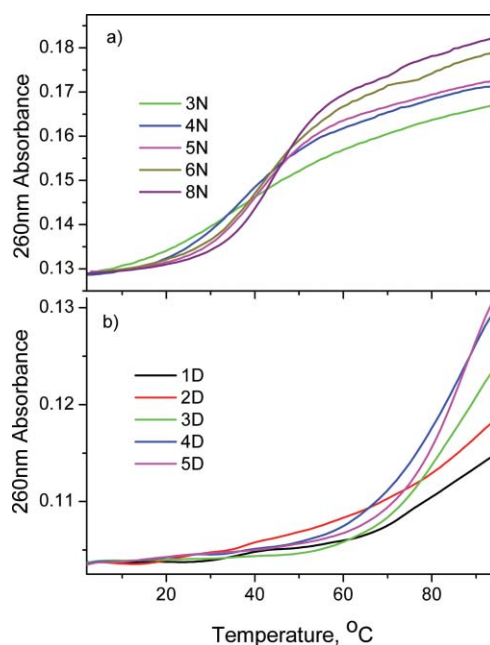


Fig. 4 Thermal dissociation profiles for (a) nicked dumbbells **nN** ($n = 3-8$) and (b) dumbbells **nD** ($n = 1-5$) determined at 260 nm (ca. $5 \mu\text{M}$ conjugate, 10 mM sodium phosphate buffer).

between the two **SA** chromophores. The sign and intensity of these bands is dependent upon the length of the base pair domains, as previously observed for the capped hairpins.² The CD bands in the $200-290 \text{ nm}$ spectral region are attributed to coupling between the dA–dT base pairs.⁸ The intensity and structure of these CD bands increase with the length of the base pair domain. These changes are most noticeable for the shorter base pair domains and become relatively insignificant for base pair domains consisting of four or more dA–dT base pairs.

Molecular dynamics simulations

Minimized structures for the nicked dumbbells and dumbbells were calculated using the AMBER force field as previously described for the capped hairpin structures.⁹ The Amber 7.0 program suite was used to run molecular dynamics simulations in the explicit water and no added salt.¹⁰ The total simulation time

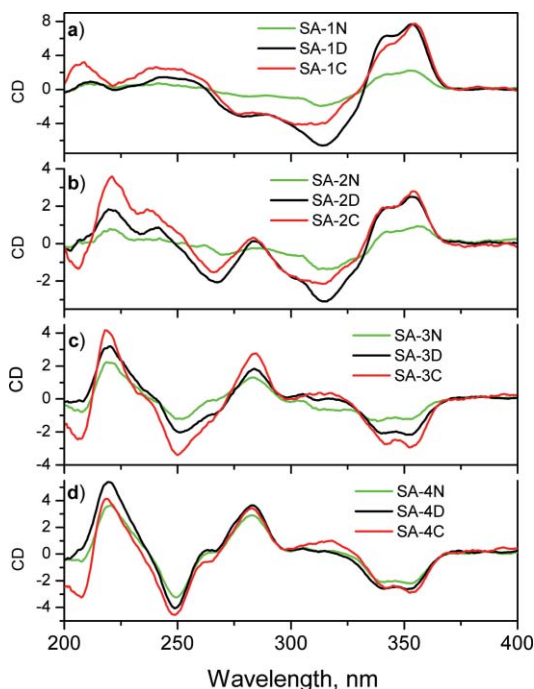


Fig. 5 CD spectra of nicked dumbbells nN , dumbbells nD , and capped hairpins nC , $n = 1-4$ ($5 \mu\text{M}$ conjugate, 10 mM sodium phosphate buffer, 0.1 M NaCl).

for each conjugate structure was 4.0 ns with a time step of 2 fs . The mass-weighted root mean square deviations (RMSd) do not have large fluctuations with respect to the MD-averaged structure, indicating that the simulations have reached equilibrium. RMSd values increase with the length of the DNA base pair domain, as expected for a flexible DNA structure. Minimized structures for **6N** and **6D** are shown in Fig. 6. These structures represent local minima arrived at from idealized B-DNA input structures.¹¹ The average angle and distance between the stilbene long axes of the nicked dumbbells and dumbbells are reported in Table 2, along with published data for the capped hairpins.²

Discussion

Synthesis and structure of the nicked-dumbbells

Nicked dumbbells possessing SA linkers (Chart 1c) were prepared by methods similar to those employed for the preparation of

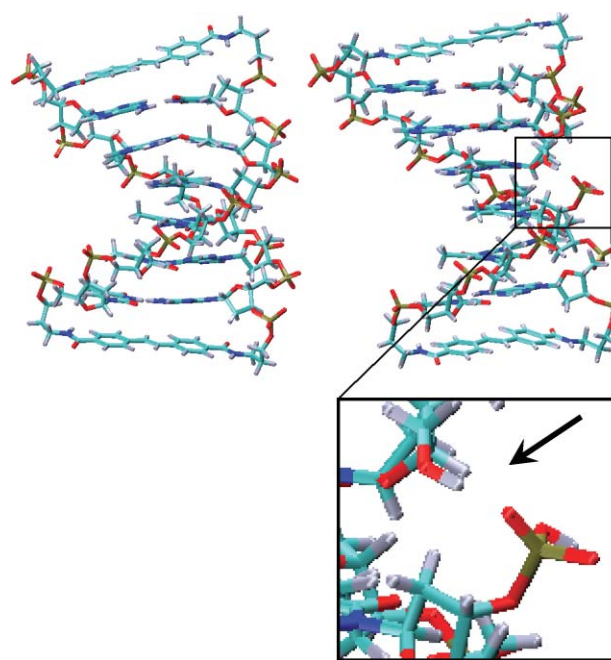


Fig. 6 Minimized structures for **6D** (left) and **6N** (right, with nick shown in inset) obtained from molecular dynamics simulations.

capped hairpins having SA linkers.² Based on the observation of hyperchromism upon heating (Fig. 4a) and the appearance of the CD spectra (Fig. 5), SA-linked nicked dumbbells possessing three or more dA–dT base pairs appear to adopt folded structures at low temperatures, similar to those of the analogous capped hairpins. Even the shortest nicked dumbbells possessing only one or two base pairs display weak SA–SA exciton coupling in their CD spectra (Fig. 5), indicative of partially ordered structures.²

The melting temperatures of the SA-linked nicked hairpins are distinctly lower than those previously reported for the analogous capped hairpins (Table 1).² For example, the nicked hairpin with a 5-mer base pair domain has a $T_m = 40 \text{ }^\circ\text{C}$, whereas the capped hairpin with a 5-mer base pair domain has a $T_m = 70 \text{ }^\circ\text{C}$. The values of T_m for the nicked dumbbells having 3 or more base pairs are not strongly dependent upon the number of base pairs, as previously observed for the capped hairpins.² This suggests that base pair dissociation is initiated at the point of the nick and proceeds toward the hairpin linkers and that a nick between thymine bases is more susceptible to base pair disruption than is the capped end of a hairpin. It is

Table 2 Calculated dihedral angles and distances between terminal SA chromophores in nicked dumbbell, dumbbell, and capped hairpin conjugates

n^a	Dihedral angle/degrees			Distance/Å		
	nN	nD	nC	nN	nD	nC
1	19 ± 11	36 ± 14	33 ± 12	7.4 ± 0.3	7.5 ± 0.4	7.2 ± 0.3
2	80 ± 10	70 ± 12	59 ± 13	10.6 ± 0.4	10.7 ± 0.4	11.7 ± 0.7
3	100 ± 11	113 ± 8	102 ± 18	14.5 ± 0.6	14.2 ± 0.5	14.3 ± 0.7
4	139 ± 14	142 ± 12	131 ± 15	17.7 ± 0.6	17.7 ± 0.6	17.7 ± 0.6
5	147 ± 17	163 ± 9	162 ± 8	20.9 ± 0.5	20.8 ± 0.5	21.0 ± 0.5
6	209 ± 11	209 ± 10	213 ± 10	24.3 ± 0.7	24.3 ± 0.7	24.2 ± 0.6
8	271 ± 13	256 ± 13	257 ± 12	30.9 ± 0.7	30.9 ± 0.7	30.8 ± 0.6
Average ^b	34 ± 2	32 ± 2	35 ± 1	3.38 ± 0.02	3.36 ± 0.02	3.36 ± 0.03

^a Number of base pairs separating the SA chromophores. ^b Average angle and distance per base pair.

interesting to note that values of T_m for **6N** and **8N** in the presence of 0.1 M NaCl are somewhat higher than the values for SA-linked hairpins with stems consisting of 3 and 4 dA–dT base pairs at the same salt concentration (Table 1).¹ Thus base-stacking between the two segments of the nicked dumbbell provides protection from thermal dissociation.

Information about the structures of the SA-linked nicked dumbbells can be inferred from their CD spectra (Fig. 5). The bisignate CD bands observed in the 290–360 nm spectral region are attributed to exciton-coupling between the two SA chromophores.¹² The rotational strength of an isolated CD transition is determined by the imaginary part of the dot product between the electronic and magnetic transition dipoles. In the case of small Davydov splitting between chromophores whose transition dipoles (μ_i and μ_j) are perpendicular to the distance vector R_{ij} , the complex expression for the rotational strength can be simplified to provide eqn (1),

$$\Delta\epsilon \approx \pm \frac{\pi}{4\lambda} \mu_i^2 \mu_j^2 R_{ij}^{-2} \sin(2\theta) \quad (1)$$

where $\Delta\epsilon$ is the molar CD ($M^{-1} \text{ cm}^{-1}$) and λ is the wavelength.² According to eqn 1, the EC–CD intensity should display a R_{ij}^{-2} dependence and have maximum intensity when the dihedral angle θ between the chromophore transition dipoles is 45° or 135° (with an inversion in sign) but zero intensity when they are parallel or perpendicular. The signs of the EC–CD bands for the nicked dumbbells are similar to those for the analogous capped hairpins or dumbbells, however the band intensities are weaker for the shortest dumbbells, which have 1–3 A–T base pairs. The CD band intensities both in the long wavelength region and in the 200–290 nm region attributed to base pair exciton coupling are similar for nicked dumbbells, capped hairpins, and dumbbells having four or more base pairs (Fig. 5).

Additional information about the structures of the SA-linked nicked dumbbells is provided by their calculated structures obtained from molecular dynamics simulations (Table 2). Even the shortest of the nicked dumbbells is found to have a compact folded structure in which the linkers are approximately parallel. The weak EC–CD spectra for the nicked dumbbells having short base pair domains are consistent with their calculated SA–SA dihedral angles (eqn 1), which are closer to 0° (**1N**) or 90° (**2N**) than are the calculated angles for the corresponding dumbbells or capped hairpins.

The calculated structure of **6N** shown in Fig. 6 displays π -stacking of the base pairs on either side of the nick. This is consistent with the X-ray crystal structure of a ternary nicked duplex system consisting of the 12-mer template d(CGCGAAAACGCG) and the 6-mers d(CGCGTT) and d(TTCGCG), which displays normal B-DNA geometry with stacking of the dT–dT bases on either side of the nick.¹³

Synthesis and structure of the dumbbells

Both enzymatic and chemical methods have been reported for the formation of dumbbell structures having non-nucleotide linkers *via* the ligation of nicked dumbbells.¹⁴ Letsinger and co-workers reported a chemical ligation procedure for the synthesis of dumbbells, including a mini-dumbbell possessing two G–C base pairs connected by SA linkers. These dumbbells possess an unnatural phosphorothioate linker.^{15,16} Cyanogen bromide has

been widely used for the chemical ligation of nicked duplexes and dumbbells.¹⁷ Chemical ligation of nicked dumbbells or duplexes requires that the reactive groups be in reasonably close proximity, as is the case for the 5'-hydroxyl and 3'-phosphate groups in the minimized structure for **6N** shown in Fig. 6. Chemical ligation of **1N** requires reaction of the 3'-phosphate with the free hydroxyl group of the capping SA. The high ligation yield for **1N** is indicative of a folded, π -stacked structure for **1N** and expands the scope of CNBr ligation to un-natural linkages.

The dumbbells have substantially higher values of T_m than the corresponding nicked dumbbells (Table 1). The values of T_m for the SA-linked capped hairpins are intermediate between those of the nicked dumbbells and dumbbells. As previously reported by Herrlein and Letsinger,¹⁵ even very short mini-dumbbells are highly resistant to base-pair dissociation. We note that the values of T_m for the SA-linked dumbbells actually decrease slightly with the length of the base pair domain, suggesting that melting may occur from the interior rather than the ends of the longer base pair domains.

As previously noted, the long-wavelength CD bands attributed to SA–SA exciton coupling are much stronger for the SA-linked dumbbells with short base pair domains than for the corresponding nicked-dumbbells (Fig. 5). However, the sign and intensity of the CD bands of the dumbbells and capped hairpins display a similar dependence on the length of the base pair domain, in accord with our earlier proposal that the capped hairpins adopt structures in which the capping group is aligned with the adjacent base pair in a manner that provides optimum stabilization for the capped structure.² Solution ¹H NMR studies further support a restricted π -stacked geometry for a stilbene-capped duplex structure adjacent to a long base pair domain.¹⁸

The calculated structure of **6D** displays distinct curvature (Fig. 6), as is commonly observed for A-tracts possessing 3–7 dA residues.¹⁹ Several models have been proposed to explain the A-tract curvature. McLaughlin *et al.* have recently reported that A-tract curvature is strongly mediated by metal ion binding in the minor groove and can be eliminated by deletion of a thymine carbonyl oxygen near the middle of the A-tract.²⁰ The presence of a mid-strand nick also reduces the extent of curvature in the calculated structure for **6N** (Fig. 6).

The calculated end-to-end distances and average rise for the nicked dumbbells, dumbbells, and capped hairpins (Table 2) are similar and relatively independent of the length of the base pair domain. The calculated dihedral angles between SA long axes are also similar for the three types of conjugate having three or more dA–dT base pairs. It is interesting to note that the calculated fluctuations in the average dihedral angles between SA chromophores do not increase as the base pair domains become longer (Table 2). This suggests that an increase in twisting angle in one part of the duplex may be compensated for by a decrease in another part.

Electronic interactions in base pair domains

The 260 nm absorption band attributed to the A–T base pairs in SA-linked nicked dumbbells and dumbbells undergoes a blue shift as the number of base pairs is increased from 1 to 4, but little further shift with additional base pairs (Fig. 3). A similar shift is observed for the SA-linked capped hairpins.² These observations

establish that the UV band shape and maximum for A-tracts possessing four or more base pairs are independent of the length of the base pair domain.

The CD spectra of the nicked dumbbells, dumbbells, and capped hairpins in the A–T base pair region (200–290 nm) display similar dependence upon the length of the base pair domain (Fig. 5). The presence of characteristic CD maxima near 220 nm and 280 nm and minimum near 250 nm is well-established in conjugates having four or more base pairs. The most noticeable domain-length dependent change is the appearance of a shoulder or maximum near 260 nm. Appearance of a distinct shoulder requires 4 base pairs and a resolved 260 nm band maximum requires 6 base pairs for the SA-linked conjugates. The relative intensity of the 256 nm band in poly(dA) sequences is known to increase with the length of the A-tract in complementary poly[d(A_nT_n)] duplexes.⁸ A shoulder is observed for poly[d(A₅T₅)], but not for poly[d(A₃T₃)] and a resolved band maximum is observed for poly[d(A₉T₉)].

Concluding remarks

The use of CNBr for the chemical ligation of nicked dumbbells extends the scope of this widely applicable method to the synthesis of mini-dumbbells possessing non-nucleotide SA linkers with A-tract base pair domains. The dumbbell 1N possesses a single A–T base pair and is the shortest dumbbell reported to date. The success of the ligation procedure is a consequence of the compact folded structures of the precursor nicked dumbbells in which the reactive 3'-phosphate and 5'-hydroxyl groups can readily approach each other. We are currently extending the use of CNBr ligation for the preparation of mini-dumbbells having other non-nucleotide linkers.²¹

The thermal stability of the nicked dumbbells is slightly greater than that of hairpins having half the number of base pairs, indicating that π -stacking between bases on either side of the nick imparts additional stability to the nicked dumbbell. The exceptional stability of the mini-dumbbells suggests that melting of the nicked dumbbells is initiated at the nick. Molecular modeling of both the nicked dumbbell and dumbbell structures indicates that their base pair domains adopt normal B- or B'-DNA structures.

The regular B-DNA structure of the mini-dumbbells makes them well-suited for studies of distance and angular dependence of electronic interactions between the linker chromophores. As seen in Fig. 5, the CD spectra of the shortest dumbbells display stronger exciton coupling between the stilbene linkers than is the case for either the nicked dumbbells or capped hairpins. As will be reported elsewhere, the electronic excited states of the mini-dumbbells undergo distance-dependent symmetry-breaking to yield charge-separated states with positive and negative charges on the two stilbene linkers.

Experimental

Materials

The preparation of *trans*-*N,N'*-bis(3-hydroxypropyl)stilbene-4,4'-dicarboxamide (SA) and its conversion to the mono-protected, mono-activated diol by sequential reaction with 4,4'-dimethoxytrityl chloride and with 2-cyanoethyl diisopropylchlorophosphoramidite have been elsewhere described.¹ Nicked

Table 3 MALDI-TOF mass spectral data

conjugate ^a	Calcd.	Observed
1N	1524.25	1524.11
1D	1506.24	1507.08
2N	2141.65	2141.16
2D	2123.64	2124.59
3N	2759.05	2757.64
3D	2741.04	2739.13
4N	3376.45	3373.26
4D	3358.44	3360.55
5N	3993.85	3997.44
5D	3975.84	3973.58

^a Conjugate structures are shown in Chart 1.

dumbbell sequences were synthesized by means of conventional phosphoramidite chemistry using a Millipore Expedite DNA synthesizer following the procedure of Letsinger and Wu¹ starting from 3'-phosphate CPG as solid support. Following synthesis, the conjugates were first isolated as trityl-on derivatives by reverse phase (RP) HPLC, then detritylated in 80% acetic acid for 30 min, and repurified by RP-HPLC as needed. RP HPLC analysis was carried out on a Dionex chromatograph with a Hewlett-Packard Hypersil ODS-5 column (4.6 × 250 mm) and a 1% gradient of acetonitrile in 0.03 M triethylammonium acetate buffer (pH 7.0) with a flow rate of 1.0 mL min⁻¹. Gels were run using 20% PAGE containing 8.3M urea in 1 × TBE buffer.

Typical ligation procedure⁶

45 μ L of 10⁻⁴ M nicked dumbbell in 250 mM MES buffer with 20 mM Mg²⁺ was denatured at 95 °C for 5 min and allowed to cool slowly to room temperature. It was then stored in 4 °C refrigerator overnight. The ligation reaction was carried out by adding 5 μ L of 5 M CNBr in anhydrous acetonitrile to the DNA solution at 0 °C. After 5 min, 0.5 mL of ice cold 2% LiClO₄ was added and the reaction was kept in dry ice for at least 0.5 h. The suspension was then centrifuged, washed by cold acetone, and the white pellet at the bottom of the tube was dried in air or in SpeedVac before subject to further purification (PAGE or HPLC). Molecular weights of all nicked dumbbells and dumbbell conjugates were determined by means of MALDI TOF mass spectroscopy following desalting. Mass spectral data is provided in Table 3.

Electronic spectroscopy

UV spectra and thermal dissociation profiles were determined using a Perkin-Elmer Lambda 2 UV spectrophotometer equipped with a Peltier sample holder and a temperature programmer for automatically increasing the temperature at the rate of 0.5 °C min⁻¹. Circular dichroism spectra were obtained using a JASCO J-715 Spectropolarimeter equipped with a Peltier sample holder and temperature controller.

Acknowledgements

Financial support for this research was provided by grants from the National Science Foundation (CHE-0400663 to FDL, CHE-0628130 to FDL and AFOSR DURINT to GCS).

References

- 1 R. L. Letsinger and T. Wu, *J. Am. Chem. Soc.*, 1995, **117**, 7323–7328.
- 2 F. D. Lewis, L. Zhang, X. Liu, X. Zuo, D. M. Tiede, H. Long and G. S. Schatz, *J. Am. Chem. Soc.*, 2005, **127**, 14445–14453.
- 3 F. D. Lewis, X. Liu, Y. Wu and X. Zuo, *J. Am. Chem. Soc.*, 2003, **125**, 12729–12731.
- 4 F. D. Lewis, L. Zhang and X. Zuo, *J. Am. Chem. Soc.*, 2005, **127**, 10002–10003.
- 5 F. D. Lewis, Y. Wu, L. Zhang, X. Zuo, R. T. Hayes and M. R. Wasielewski, *J. Am. Chem. Soc.*, 2004, **126**, 8206–8215; F. D. Lewis, H. Zhu, P. Daublain, T. Fiebig, M. Raytchev, Q. Wang and V. Shafirovich, *J. Am. Chem. Soc.*, 2006, **128**, 791–800.
- 6 S. Carriero and M. J. Damha, *Org. Lett.*, 2003, **5**, 273–276.
- 7 F. D. Lewis, T. Wu, X. Liu, R. L. Letsinger, S. R. Greenfield, S. E. Miller and M. R. Wasielewski, *J. Am. Chem. Soc.*, 2000, **122**, 2889–2902.
- 8 S. R. Gudibande, S. D. Jayasena and M. J. Behe, *Biopolymers*, 1988, **27**, 1905–1915.
- 9 W. D. Cornell, P. Cieplak, C. I. Bayly, I. R. Gould, K. M. Merz, D. M. Ferguson, D. C. Spellmeyer, T. Fox, J. W. Caldwell and P. A. Kollman, *J. Am. Chem. Soc.*, 1996, **118**, 2309–2309.
- 10 D. A. Case, D. A. Pearlman, J. W. Caldwell, T. E. C. III, J. Wang, W. S. Ross, C. L. Simmerling, T. A. Darden, K. M. Merz, R. V. Stanton, A. L. Cheng, J. J. Vincent, M. Crowley, V. Tsui, H. Gohlke, R. J. Radmer, Y. Duan, J. Pitera, I. Massova, G. L. Seibel, U. C. Singh, P. K. Weiner and P. A. Kollman, *AMBER 7*, 2002, San Francisco.
- 11 S. Arnott, P. J. Campbell-Smith and R. Chandrasekaran, in *Handbook of Biochemistry and Molecular Biology*, CRC Press, Cleveland, OH, 3rd edn, 1976, pp. 411–422.
- 12 N. Harada and K. Nakanishi, *Circular dichroic spectroscopy: exciton coupling in organic stereochemistry*, University Science Books, Mill Valley, CA, 1983.
- 13 J. C. Aymami, Miquel Van DerMarel, Gijs A. VanBoom, Jacques H. Wang, Andrew H. J. Rich and Alexander, *Proc. Natl. Acad. Sci. U. S. A.*, 1990, **87**, 2526–2530.
- 14 G. W. Ashley and D. M. Kushlan, *Biochemistry*, 1991, **30**, 2927–2933; D. Erie, N. Sinha, W. Olson, R. Jones and K. Breslauer, *Biochemistry*, 1987, **26**, 7150–7159; C. S. Lim and C. A. Hunt, *Nucleosides Nucleotides*, 1997, **16**, 41–51; A. P. Silverman and E. T. Kool, *Chem. Rev.*, 2006, **106**, 3775–3789.
- 15 M. K. Herrlein and R. L. Letsinger, *Angew. Chem., Int. Ed. Engl.*, 1997, **36**, 599–601.
- 16 M. K. Herrlein, J. S. Nelson and R. L. Letsinger, *J. Am. Chem. Soc.*, 1995, **117**, 10151–10152.
- 17 S. A. Kuznetsova, I. N. Merenkova, I. E. Kanevsky, Z. A. Shabarova and M. Blumenfeld, *Antisense Nucleic Acid Drug Dev.*, 1999, **9**, 95–100; Z. A. Shabarova, O. A. Fedorova, N. G. Dolinnaya and M. B. Gottikh, *Origins Life Evol. Biosphere*, 1997, **27**, 555–566.
- 18 J. Tuma, R. Paulini, J. A. Rojas Stutz and C. Richert, *Biochemistry*, 2004, **43**, 15680–15687.
- 19 J. G. Nadeau and D. M. Crothers, *Proc. Natl. Acad. Sci. U. S. A.*, 1989, **86**, 2622–2626.
- 20 Meena Z Sun, C. Mulligan and L. W. McLaughlin, *J. Am. Chem. Soc.*, 2006, **128**, 11756–11757.
- 21 L. Zhang and A. Karaba, unpublished results.